Available online at www.sciencedirect.com
SCIENCE DIRECT®
Journal of Solid State Chemistry 178 (2005) 3605–3614
JOURNAL OF SOLID STATE CHEMISTRY
www.elsevier.com/locate/jssc

Structural and magnetic properties of perovskite $Ca_3Fe_2WO_9$

Sergey A. Ivanov[a], Sten Gunnar Eriksson[b,*], Roland Tellgren[c], Häkan Rundlöf[c]

[a]Department of Inorganic Materials, Karpov' Institute of Physical Chemistry, Vorontsovo pole, 10 103064 Moscow K-64, Russia
[b]Department of Environmental Inorganic Chemistry, Chalmers University of Technology, SE-412 96, Göteborg, Sweden
[c]Department of Materials Chemistry, The Ångstrom Laboratory, Box 538, University of Uppsala, SE-751 21, Uppsala, Sweden

Received 25 May 2005; received in revised form 12 July 2005; accepted 18 August 2005
Available online 7 November 2005

Abstract

A complex perovskite with composition $Ca_3Fe_2WO_9$ has been synthesised, and the temperature evolution of nuclear and magnetic structures investigated by neutron powder diffraction. It was shown that at room temperature this compound adopts a monoclinic perovskite structure belonging to space group $P12_1/n1$ ($a = 5.4180(5)$ Å, $b = 5.5093(5)$ Å, $c = 7.7031(7)$ Å), $\beta = 90.04(2)^\circ$). The partial *B*-site ordering, of the Fe^{+3} and W^{+6} cations, at (2*c*) and (2*d*) sites was determined. At low temperatures the magnetic diffraction peaks were registered and a possible model for the magnetic structure was proposed in accordance with the ferrimagnetic properties of the title compound. The magnetic structure is defined by a propagation vector $k = (1/2, 1/2, 0)$ and can be described as an array of ferromagnetic (20−1) layers, which couple antiferromagnetically to each other. All the Fe moments within a layer are aligned parallel (or anti-parallel) to the *c*-axis. The structural and magnetic features of this compound are discussed and compared with those of some other quaternary oxides $A_3Fe_2WO_9$ (A = Ba, Sr, Pb).

Keywords: Magnetoelectrics; Neutron scattering; Crystal structure; Magnetic structure

1. Introduction

In the last several years, there has been a revival of interest in the search and understanding of so-called magnetoelectric materials [1,2]. Magnetoelectrics are the substances where electrical and magnetic orders coexist in the same phase and are coupled within a certain temperature interval [3]. The application of an electric/magnetic field to the magnetoelectric material is expected to control spontaneous magnetisation/polarisation by means of a magnetoelectric interaction. Therefore, this class of multifunctional and smart compounds has been an interesting subject not only from the viewpoint of fundamental solid-state physics, which is rich and fascinating, but also for possible modern applications [4,5]. However, ferroelectricity and magnetism hardly coexist due to the structural competition and the chances of the occurrence of magnetoelectrics are very low [1,2]. Difficulties arise mainly due to the fact that in the perovskite structure ferroelectricity appears only in non-centrosymmetric phases, which is in contrast to magnetic cations, as they prefer a centrosymmetric surrounding. Until now only a few compounds have been reported to exhibit both ferroelectricity and ferromagnetism in the same phase [6]. The known ferromagnetic ferroelectrics have, unfortunately, been studied with different degrees of thoroughness and technical applications of these materials are severely limited. In many cases data only on the temperatures of ferroelectric and magnetic phase transitions T_{CE} and T_{CM} are available. Sparse data are available on their atomic and magnetic structures. Of particular importance is the development of strategies for search of magnetoelectrics which display magnetic and ferroelectric ordering at room temperature.

A search for the magnetoelectric perovskites showing ferromagnetism and ferroelectricity simultaneously in the same phase began in the 1950s with the substitution of

*Corresponding author. Fax: +46 31 772 2857.
E-mail addresses: ivan@cc.nifhi.ac.ru (S.A. Ivanov), stene@inoc.chalmers.se, stene@chem.gu.se (S.G. Eriksson), rte@mkem.uu.se (R. Tellgren).

0022-4596/$ - see front matter © 2005 Published by Elsevier Inc.
doi:10.1016/j.jssc.2005.08.012

diamagnetic cations by paramagnetic ones in the *B*-sublattice [7]. During the same period it was also found that the presence of diamagnetic ions with noble gas configuration (W^{6+} for example) would be beneficial for ferroelectric properties to occur in these complex metal oxides [8]. When the *B*-sites in complex perovskite oxides are partly occupied by transition metal cations, the magnetic properties are strongly influenced by the ordering of the *B*-site ions.

These studies, however, have mainly been focused on the effect of a systematic change of size and oxidation state of A and *B* cations upon the magnetic and dielectric properties. Such focused attention has not yet been paid to the structural aspects of these perovskites and their crystal structures. However, precise structural studies are required to unravel the complex composition/structure/properties relationships in magnetoelectric perovskites. The present work is a part of our comprehensive crystallochemical study of magnetoelectric perovskites. Much of our recent research has been concerned with the dielectric and magnetic properties of iron-based perovskite-type compounds [9–13], which have a great interest in many applied and fundamental areas of solid-state chemistry, physics and advanced materials science. These oxides exhibit rather unusual magnetic and dielectric properties, leading to a number of original materials. Synthesised and investigated for the first time a long time ago [14,15], and forgotten for a few decades, these compounds have regained much interest, which arises from the prospects of finding half-metallic oxides with high Curie temperatures.

We focus our attention on a perovskite-type oxide $Ca_3Fe_2WO_9$ (CFWO) as a possible new magnetoelectric compound where we may expect that two coupled degrees of freedom based on a local off-centred lattice distortion and on electron spin will take place. Preparation of CFWO has been reported on several occasions; however, no structural determination has been performed [14,15]. The previous experimental studies gave us some indicators that this compound may show some combination of magnetic and ferroic properties. The details of this coexistence, however, still remain an open question and have to our knowledge never been reported. The careful dielectric measurements of CFWO were made difficult by the high conductivity of the specimen [14]. Nevertheless, it was conceived that a possible antiferroelectric ordering in CFWO may occur.

In this situation, neutron powder diffraction (NPD) data may help to determine the factors that are responsible for magnetic interactions in this material. The advantages of neutron diffraction over X-ray diffraction for structural studies of complex metal oxides (containing light oxygen anions in the presence of heavy cations) are well known. X-ray experiments are not able to give precise quantitative information about the order parameter of the phase transition, as it is mainly related to the tilting and distortion of the oxygen sublattice. In this work, we report the results of a NPD study of CFWO in the temperature range 10–1000 K. The objective of the present research was to determine the temperature evolution of structural characteristics of CFWO with a particular emphasis on the magnetic structure.

2. Experimental

A high-quality polycrystalline sample of CFWO was prepared by a conventional solid-state sintering reaction. As starting materials, $CaCO_3$, Fe_2O_3 and WO_3 were used. They were first weighed in order to obtain appropriate metal ratios, mixed together and ground in an agate mortar to a uniform paste. Acetone was added as a grinding aid. The sample was pressed into a pellet at 100 MPa and then heated at 900 °C (8 h) followed by 1200 °C for 2 days in air with several internal grindings and pellet-making steps in between. Phase identification of the obtained sample was characterised by X-ray powder diffraction (XRD) (URD-63 diffractometer, Ni-filtered Cu K_α-radiation). The lattice parameters were calculated using silicon powder (NBS 640b) as an internal standard. The prepared sample was pure single phase and the XRD pattern shows only diffraction lines characteristic of perovskite-type structure. Cation composition of the CFWO sample was determined by X-ray energy-dispersive spectrometry (EDS) and by using well-characterised standards. Electron probe microanalysis shows that the studied sample contains close to the expected cation ratio, which was estimated as $Ca_{2.98(2)}Fe_{2.01(1)}W_{1.01(1)}O_9$. The size of the crystallites in the obtained powder does not exceed 10–15 μm.

Medium-resolution NPD data were collected at the Swedish Research reactor R2 at Studsvik with a Huber two-circle diffractometer equipped with an array of 35 ^{3}He detectors. The intensity from each detector was statistically analysed and summed. A monochromator system with two copper crystals (220) in a parallel arrangement was used. The wavelength was 1.470(1) Å and the neutron flux at the sample position approximately 10^6 neutrons $cm^{-2} s^{-1}$. Diffraction patterns were registered at temperatures 10, 100, 200, 300, 380, 500, 700 and 1000 K. The powder sample of CFWO (approximately 2 g) was loaded into a thin-walled vanadium container and held in a cryostat. Absorption effects were later corrected for in the Rietveld refinements using the experimentally determined value $\mu R = 0.0903$. The step-scan covered a 2θ-range from 4.00° to 139.92° with a step-length 0.08°, and with each data collection lasting approximately 15 h. The diffraction data were refined by the Rietveld method using the FULLPROF 2000 software [16]. Scattering lengths and form factors for Fe^{3+} were taken from the program library. The diffraction peaks were described by a pseudo-Voigt function and a Lorentzian contribution to the Gaussian peak shape was refined. Peak asymmetry correction was made for angles below 35° in 2θ. The background was described by a six-parameter polynomial. During the refinements, the two octahedrally coordinated metal cations (Fe and W) were allowed to vary their proportions

on the two possible metal sites. Each structural model was refined to convergence and the best result was chosen on the basis of agreement factors and stability of the refinement.

Magnetic susceptibilities were measured with a Quantum Design SQUID magnetometer at an applied field of 10 Oe in the temperature range 5–400 K. Zero field cooled measurements (ZFC) were performed by cooling the samples to 10 K, applying the field, and measuring the magnetisation as the samples were warmed.

The ^{57}Fe Mössbauer transmission spectra of CFWO were obtained by means of a standard constant acceleration spectrometer using a ^{57}Co/Pd source.

3. Results

In Fig. 1 the temperature dependence of the magnetisation of CFWO is shown. The temperature derivative of the magnetisation shows a minimum at 340 K. Magnetic measurements were consistent with a ferrimagnetic ordering with a magnetisation value that is relatively small (0.01 μ_B/Fe). A Fe^{3+} charge state for the iron coordinated octahedrally has been clearly confirmed by the isomer shift (0.39(1) mm/s at 100 K) and internal magnetic field (470(10) kOe at 100 K) determined by ^{57}Fe Mössbauer spectroscopy. Within the statistical uncertainty of the spectra, no Fe^{2+} cations exist in the sample. Mössbauer spectra of CFWO at selected temperatures are shown in Fig. 2. The well-developed doublet, which was obtained above the magnetic transition temperature, indicates a paramagnetic state (quadrupole splitting at 300 K is 0.87(2) mm/s) (Fig. 2a), and spectra taken below this temperature distinguish a prevailing sextet and show the existence of magnetic ordering (Fig. 2b). This sextet is consistent with most low-temperature spectra obtained for magnetically ordered double perovskites [17,18]. The two

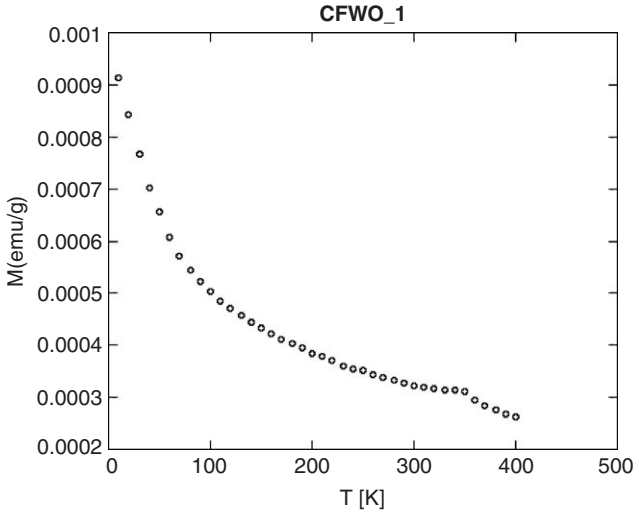

Fig. 1. Temperature dependence of the magnetisation for $Ca_3Fe_2WO_9$ ($H = 10$ Oe).

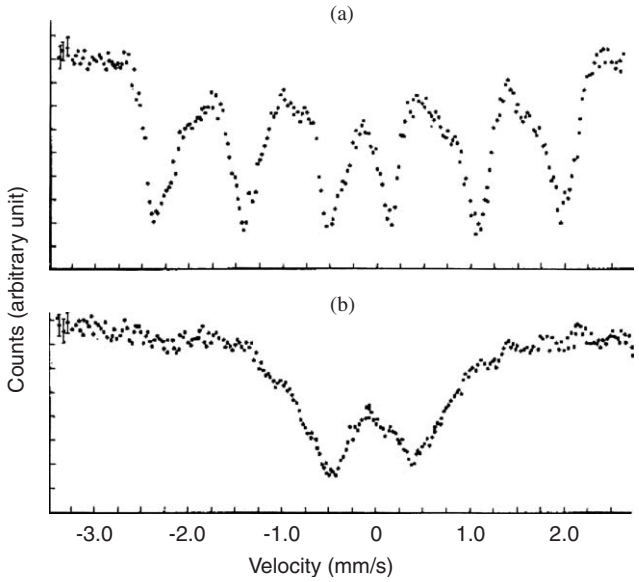

Fig. 2. ^{57}Fe Mössbauer spectra of $Ca_3Fe_2WO_9$ at selected temperatures: (a) 10 K, (b) 350 K.

Fe sites with a different local environment are seen in the Mössbauer spectra at all registered temperatures. These spectra for the paramagnetic and ferrimagnetic states are expected, since two different crystallographic positions are occupied by Fe in the partly *B*-site ordered monoclinic $P12_1/n1$ structure of CFWO. Extended details of the description of hyperfine structure of CFWO will be published elsewhere.

XRD data confirmed the CFWO sample to be single phase. Powder patterns of CFWO could be readily identified as representing a perovskite-related phase. The first 25 peaks were used in the indexing program NTREOR [19] and the room temperature diffraction pattern could be indexed on the basis of an orthorhombic unit cell. The occurrence of a set of systematic absences suggested space group *Pnma*. For this space group only a single mixed *B*-site for cations is allowed. By contrast, the room temperature NPD pattern could not be indexed within the same orthorhombic cell. Indeed, the splitting of some reflections and violation of the systematic absences of space group *Pnma* indicated a reduction of the symmetry to monoclinic. Analysis of the systematic absences $h0l : h + l = 2n + 1$ and $0k0 : k = 2n + 1$ was indicative of space group $P12_1/n1$. This reduction in symmetry opened up for the possibility of two distinct sites for the different *B*-type cations. Initially the fractional occupancies of Fe and W were defined as 67% Fe and 33% W, in accordance with the results of the chemical analysis. The Fe/W distribution between the two distinct *B*-sites was allowed to vary with the constraint that the 2:1 composition ratio was maintained. The site occupancy refined by the Rietveld method supports the chosen structural model and indicates some degree of ordering between Fe and W at the 2*c* and 2*d* sites. The contrast in scattering lengths for Fe and W allows the

distribution of these cations between the two positions to be determined with a high accuracy. Refinements of the site occupancy factors of the oxygen atoms did not reveal significant changes from full occupancy (within three standard deviations) and was therefore fixed at unity. The final Fourier difference-synthesis calculation, using (F_o–F_c) neutron data, did not show any maximum. The refinement using space group $P12_1/n1$ achieves a better fit between the calculated and observed patterns than the refinement based on the orthorhombic model. At 300 K, the values of R_P, R_{WP} and R_B-factors for the orthorhombic model, which are equal to 3.18, 4.21 and 2.98, respectively, are worse than for a monoclinic one (see Table 1).

The results indicate that the crystal structure of the title compound has a partially ordered arrangement of cations on the 6-coordinated *B*-sites. The tendency to move

Table 1
Structural parameters for $Ca_3Fe_2WO_9$ at different temperatures, Space group $P12_1/n_1$, $z = 2$

Atom	Position	x	y	z	B (Å^2)	N
$T = 1000\,K$, $a = 5.4893(5)$ Å, $b = 5.5345(5)$ Å, $c = 7.7871(7)$ Å, $\beta = 90.05(2)$, $V = 236.6$ Å^3						
$R_p = 3.22$, $R_{wp} = 4.21$, $R_B = 3.36$, $\chi^2 = 1.87$						
Ca	(4*e*)	0.0015(8)	−0.0235(8)	0.2571(8)	1.66(6)	0.99(2)
Fe_1/W_1	(2*a*)	0	1/2	0	0.72(5)	0.73/0.27(1)
Fe_2/W_2	(2*b*)	1/2	0	0	0.63(5)	0.60/0.40(1)
O_1	(4*e*)	0.2067(9)	0.2078(9)	0.0415(9)	1.37(8)	0.99(1)
O_2	(4*e*)	0.2085(9)	0.2091(9)	0.4729(8)	1.28(8)	1.00(1)
O_3	(4*e*)	0.5744(9)	0.0159(9)	0.2511(9)	1.52(8)	0.99(1)
$T = 700$ K, $a = 5.4597(5)$ Å, $b = 5.5206(5)$ Å, $c = 7.7533(7)$ Å, $\beta = 90.07(2)$, $V = 233.7$ Å^3						
$R_p = 3.17$, $R_{wp} = 4.09$, $R_B = 3.31$, $\chi^2 = 1.84$						
Ca	(4*e*)	0.0034(8)	−0.0274(8)	0.2669(8)	1.51(6)	0.99(2)
Fe_1/W_1	(2*a*)	0	1/2	0	0.68(5)	0.73/0.27(1)
Fe_2/W_2	(2*b*)	1/2	0	0	0.55(5)	0.60/0.40(1)
O_1	(4*e*)	0.2075(9)	0.2088(9)	0.0450(9)	1.19(8)	0.99(1)
O_2	(4*e*)	0.2077(9)	0.2050(9)	0.4705(9)	1.11(8)	1.00(1)
O_3	(4*e*)	0.5800(9)	0.0213(9)	0.2542(9)	1.44(8)	0.99(1)
$T = 500$ K, $a = 5.4399(5)$ Å, $b = 5.5168(5)$ Å, $c = 7.7305(7)$ Å, $\beta = 90.05(2)$, $V = 231.9$ Å^3						
$R_p = 3.08$, $R_{wp} = 4.02$, $R_B = 3.25$, $\chi^2 = 1.77$						
Ca	(4*e*)	0.0050(9)	−0.0361(8)	0.2571(8)	1.36(6)	0.99(2)
Fe_1/W_1	(2*a*)	0	1/2	0	0.64(5)	0.73/0.27(1)
Fe_2/W_2	(2*b*)	1/2	0	0	0.52(5)	0.60/0.40(1)
O_1	(4*e*)	0.2043(9)	0.2024(9)	0.0373(8)	1.10(8)	0.99(1)
O_2	(4*e*)	0.2078(9)	0.2102(9)	0.4613(8)	1.03(8)	1.00(1)
O_3	(4*e*)	0.5804(8)	0.0216(8)	0.2527(9)	1.37(8)	0.99(1)
$T = 380$ K, $a = 5.4279(4)$ Å, $b = 5.5126(4)$ Å, $c = 7.7165(5)$ Å, $\beta = 90.05(2)$, $V = 230.9$ Å^3						
$R_p = 2.94$, $R_{wp} = 3.82$, $R_B = 3.07$, $\chi^2 = 1.61$						
Ca	(4*e*)	0.0085(8)	−0.0380(7)	0.2512(8)	1.18(6)	0.99(2)
Fe_1/W_1	(2*a*)	0	1/2	0	0.58(5)	0.73/0.27(1)
Fe_2/W_2	(2*b*)	1/2	0	0	0.42(5)	0.60/0.40(1)
O_1	(4*e*)	0.2090(8)	0.2091(8)	0.0458(8)	1.03(8)	0.99(1)
O_2	(4*e*)	0.2001(8)	0.2044(8)	0.4648(8)	0.98(8)	1.00(1)
O_3	(4*e*)	0.5802(7)	0.0225(7)	0.2534(7)	1.32(8)	0.99(1)
$T = 300$ K, $a = 5.4180(4)$ Å, $b = 5.5093(4)$ Å, $c = 7.7031(5)$ Å, $\beta = 90.04(2)$, $V = 229.9$ Å^3						
$R_p = 2.81$, $R_{wp} = 3.63$, $R_B = 2.56$, $\chi^2 = 1.55$, $R_{MAG} = 4.96$						
Ca	(4*e*)	0.0045(8)	−0.0402(8)	0.2489(8)	1.07(6)	0.99(2)
Fe_1/W_1	(2*a*)	0	1/2	0	0.55(5)	0.73/0.27(1)
Fe_2/W_2	(2*b*)	1/2	0	0	0.38(5)	0.60/0.40(1)
O_1	(4*e*)	0.2075(8)	0.2099(8)	0.0447(8)	0.93(8)	0.99(1)
O_2	(4*e*)	0.2014(8)	0.2034(8)	0.4627(8)	0.82(8)	1.00(1)
O_3	(4*e*)	0.5817(6)	0.0247(6)	0.2535(6)	1.21(8)	0.99(1)
Magnetic moments: $\mu Fe_1 = 3.12(8)\,\mu_B$; $\mu Fe_2 = -2.47(9)\mu_B$						
$T = 200$ K, $a = 5.4120(4)$ Å, $b = 5.5090(4)$ Å, $c = 7.6979(5)$ Å, $\beta = 90.04(2)$, $V = 229.5$ Å^3						
$R_p = 2.87$, $R_{wp} = 3.72$, $R_B = 2.44$, $\chi^2 = 1.48$, $R_{MAG} = 4.84$						
Ca	(4*e*)	0.0079(8)	−0.0407(8)	0.2496(8)	0.84(6)	0.99(2)
Fe_1/W_1	(2*a*)	0	1/2	0	0.42(5)	0.73/0.27(1)
Fe_2/W_2	(2*b*)	1/2	0	0	0.29(5)	0.60/0.40(1)

Table 1 (*continued*)

Atom	Position	x	y	z	B (Å^2)	N
O_1	(4*e*)	0.2061(8)	0.2089(8)	0.0453(8)	0.82(8)	0.99(1)
O_2	(4*e*)	0.2033(8)	0.2050(8)	0.4620(8)	0.74(8)	1.00(1)
O_3	(4*e*)	0.5805(6)	0.0226(6)	0.2528(6)	0.86(8)	0.99(1)
Magnetic moments: $\mu Fe_1 = 3.46(8)\,\mu_B$; $\mu Fe_2 = -2.84(9)\,\mu_B$						
$T = 100$ K, $a = 5.4054(4)$ Å, $b = 5.5078(4)$ Å, $c = 7.6912(5)$ Å, $\beta = 90.03(2)$, $V = 229.0$ Å^3						
$R_p = 3.01$, $R_{wp} = 3.85$, $R_B = 2.80$, $\chi^2 = 1.57$, $R_{MAG} = 3.83$						
Ca	(4*e*)	0.0083(8)	−0.0415(8)	0.2486(8)	0.76(6)	0.99(2)
Fe_1/W_1	(2*a*)	0	1/2	0	0.24(5)	0.73/0.27(1)
Fe_2/W_2	(2*b*)	1/2	0	0	0.18(5)	0.60/0.40(1)
O_1	(4*e*)	0.2059(8)	0.2094(8)	0.0469(8)	0.80(8)	0.99(1)
O_2	(4*e*)	0.2021(8)	0.2055(8)	0.4631(8)	0.72(8)	1.00(1)
O_3	(4*e*)	0.5839(6)	0.0229(6)	0.2565(6)	0.77(8)	0.99(1)
Magnetic moments: $\mu Fe_1 = 3.66(8)\,\mu_B$; $\mu Fe_2 = -3.05(9)\,\mu_B$						
$T = 10$ K, $a = 5.4052(3)$ Å, $b = 5.5084(3)$ Å, $c = 7.6901(5)$ Å, $\beta = 90.03(2)$, $V = 228.9$ Å^3						
$R_p = 3.04$, $R_{wp} = 3.86$, $R_B = 2.88$, $\chi^2 = 1.62$, $R_{MAG} = 3.47$						
Ca	(4*e*)	0.0058(8)	−0.0413(8)	0.2507(8)	0.73(6)	0.99(2)
Fe_1/W_1	(2*a*)	0	1/2	0	0.21(5)	0.73/0.27(1)
Fe_2/W_2	(2*b*)	1/2	0	0	0.15(5)	0.60/0.40(1)
O_1	(4*e*)	0.2073(8)	0.2034(8)	0.0478(8)	0.78(8)	0.99(1)
O_2	(4*e*)	0.2021(8)	0.2085(8)	0.4619(8)	0.69(8)	1.00(1)
O_3	(4*e*)	0.5832(6)	0.0234(6)	0.2555(6)	0.74(8)	0.99(1)
Magnetic moments: $\mu Fe_1 = 3.85(7)\,\mu_B$; $\mu Fe_2 = -3.23(9)\,\mu_B$						

towards an ordered structure is more likely to be determined by the difference in charge and size between the Fe^{3+} and W^{6+} cations. Table 1 specifies the refined atomic positions, isotropic temperature factors, occupancy factors and agreement factors for CFWO at the different temperatures. The quality of the fit is illustrated in Fig. 3. The selected bond lengths and angles are listed in Table 2. Interatomic distances and bond angles demonstrate that the two types of octahedra are slightly different in size, and that the true coordination number of Ca is 8. This is in agreement with [20] where it was shown theoretically that the coordination number of the *A*-site cation may vary between 8 and 12 depending on the tilt angle and the ratio between the ionic radii of the *A*- and *B*-type cations. The refinements confirm that although the sizes of Fe and W are similar the volume of the Fe_2 site is around 3% larger than that of the Fe_1 site at room temperature.

Fig. 4 shows a view of the crystal structure of CFWO. The Fe and W cations are located at alternate *B*-sites as a result of the difference between the valence charges of these cations. This kind of monoclinic structure is characterised by *B*-site cation ordering and $a^-a^-c^+$-type BO_6 octahedral tilting [21]. The anti-parallel shift of the Ca cations, approximately along the [010] monoclinic direction, often accompanies this kind of octahedral tilting. If the radius of the A-type cation is too small, the void between the B_1 and B_2 octahedra is reduced in size by tilting of the octahedra. This size-mismatch can be quantified with the help of the tolerance factor:

$$t = \langle Ca{-}O\rangle / \sqrt{2}\langle Fe{-}O\rangle.$$

Using the data of Table 2, the t value was estimated as 0.89. For comparison, for cubic perovskite $t = 1.0$ and the stability limit is usually around $t = 0.85$. CFWO is located close to this stability limit for the perovskite structure indicating the strong deviation from an ideal cubic structure, which is also confirmed by the lowering of the Ca coordination number from 12 to 8.

The monoclinic space group $P12_1/n1$ requires that the Fe_1/W_1 and Fe_2/W_2 octahedra have different tilt angles as a result of the differences in the size and distortion of each of the two polyhedra. For monoclinic perovskites the tilt angles of the two different octahedra can be calculated from atomic coordinates using the formulas derived in [22] with the assumption that regular octahedra exist (see Table 3). Here Φ denotes a rotation about (001) of the aristotype (a fourfold axis) and Ψ denotes a rotation about (110) of the aristotype (a twofold axis).

We observe that the magnitude of the tilt about the [001] axis is smaller than that about the [110] axis for CFWO.

Fig. 5 represents the evolution of the unit cell parameters for CFWO. As the monoclinic angle varies little from 90°, it is not represented. Thermal variations of the unit-cell parameters would be related to the contraction of the unit cell due to the magnetic transition at 340 K and the thermal expansion in the paramagnetic region is significantly larger than for the ferrimagnetic phase. There was no evidence of any major change in the crystal structure between 10 and 1000 K.

Two major factors will determine the arrangement of different cations at the *B*-sites in the perovskite structure.

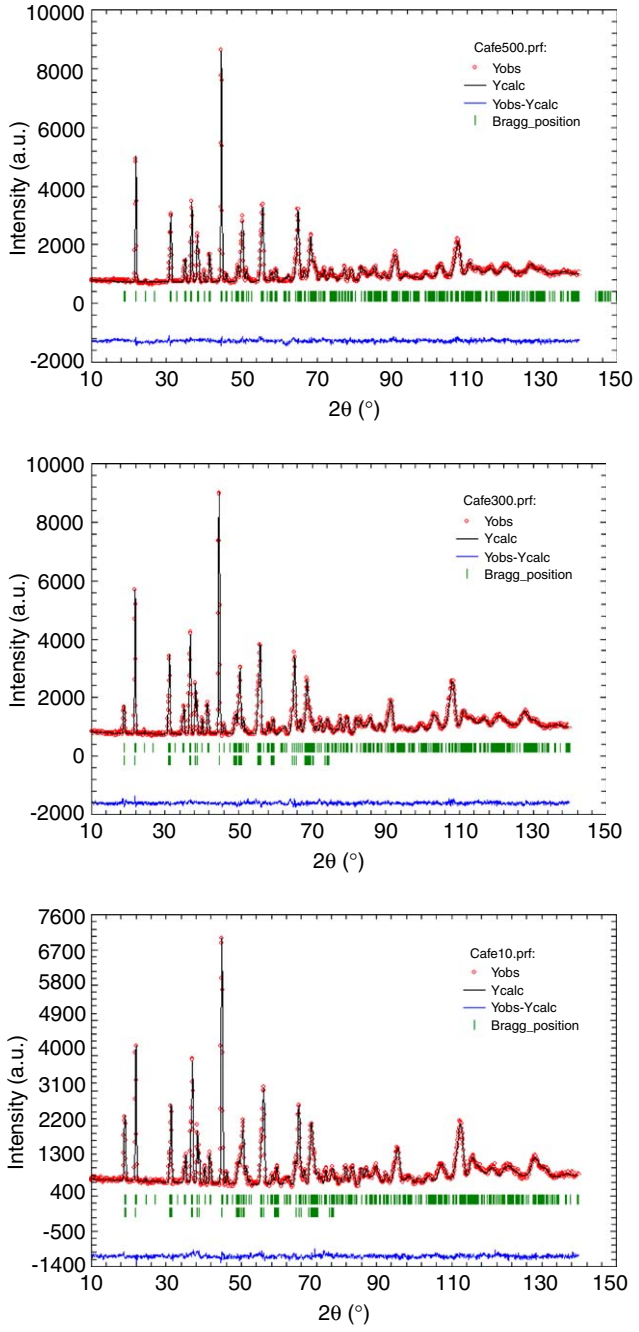

Fig. 3. The observed, calculated, and difference plots for the fit to NPD patterns of $Ca_3Fe_2WO_9$ after Rietveld refinement of the nuclear and magnetic structure at different temperatures: 500 K (a), 300 K (b) and 10 K (c).

The ions can be either ordered or statistically distributed (disordered), and the controlling factors are the difference in ionic charge and in ionic size. The ionic radii of Fe^{3+} and W^{6+} are similar and therefore we may say that this combination of cations in general favours a disordered arrangement. By using a long-range order parameter η, introduced in [23] for characterisation of the degree of order in the arrangement in B-sites within the double perovskite lattice, the ionic distribution of Fe^{3+} and W^{6+} cations for CFWO may be represented by the formula

$$Ca[Fe^{3+}_{(2+\eta)/6}W^{6+}_{(1-\eta)/6}]_{B_1}[Fe^{3+}_{(2-\eta)}W^{6+}_{(1+\eta)/6}]_{B_2}O_3.$$

The Fe^{3+} cations at the B_1-site are surrounded by six B_2-sites, which are occupied on average 60% by Fe^{3+} and 40% by W^{6+} ions on average. A Fe^{3+} cation on a B_2-site is surrounded by six B_1-sites, which are occupied on average 73% by Fe^{3+} ions and 27% by W^{6+}. The Fe^{3+} cations provide much greater internal magnetic field to the neighbouring iron sites than the W^{6+} ions, and therefore the magnetic moments are expected to differ for Fe^{3+} ions situated on B_1- and B_2-sites, respectively. From the results obtained from analysis of our NPD data, the atomic arrangement in our CFWO sample can be represented as follows:

$$Ca[Fe^{3+}_{0.367}W^{6+}_{0.133}]_{B_1}[Fe^{3+}_{0.300}W^{6+}_{0.200}]_{B_2}O_3.$$

The value of the magnetic transition temperature can be calculated following the hypothesis [23,24] that a magnetic ion, which has no magnetic neighbours or only one magnetic neighbour, does not take part in the magnetic ordering. In our case there are two magnetic sub-lattices with octahedral sites, and k_1 and k_2 are the fractions of non-magnetic ions in the sub-lattices B_1 and B_2, respectively. $E(k1)$ (or $E(k2)$) are the probabilities that a given ion of the sub-lattice B_2 (or B_1) has not more than one magnetic neighbour in the sub-lattice B_1(or B_2).

The number of magnetically active ions and the number of effective magnetic interactions per molecular unit are given as

$$N = 0.5(1-k_1)[1-E(k_2)] + 0.5(1-k_2)[1-E(k_1)],$$
$$n = 6(1-k_1)[1-E(k_2)](1-k_2)[1-E(k_1)],$$

6 is the coordination number for a cation at the B-site of the perovskite lattice. The magnetic transition temperature of our CFWO composition $T_N(k_1,k_2)$ is related to the standard Neel temperature $T_N(0,0)$ by

$$T_N(k_1,\ k_2) = \tfrac{1}{6}(n/N)T_N(0,0).$$

We take $T_N(0,0)$ as the Neel temperature of $BiFeO_3$ with perovskite structure. The comparison of the calculated (376 K) and observed (330 K) values of T_{CM} computed for our CFWO sample, on the basis of the iron content obtained from our NPD data, shows quite good agreement.

Rietveld refinement of the low-temperature structure from the data recorded at 10, 100 and 200 K showed that the $P2_1/n$ symmetry is maintained down to 10 K. NPD data from 10 to 500 K are shown in Fig. 6 and these data were used to follow the thermal evolution of the main magnetic reflections, which arise from a long-range magnetic order in the sample. Diffraction patterns collected at 10, 100, 200 and 300 K revealed the presence of additional reflections that can be indexed with integer indices in the lattice with a doubling of the a and b axes relative to the monoclinic nuclear cell; these reflections are defined by the wave vector: $k = [1/2, 1/2, 0]$. Worthwhile to

Table 2
Selected interatomic distances (Å) and angles (°) for $Ca_3Fe_2WO_9$ at the different temperatures

Bond	1000 K	700 K	500 K	380 K	300 K	200 K	100 K	10 K
Ca–O	2.475(4)	2.431(4)	2.403(4)	2.357(4)	2.363(4)	2.349(4)	2.336(4)	2.335(4)
	2.625(4)	2.595(4)	2.665(3)	2.597(3)	2.618(4)	2.605(4)	2.596(4)	2.603(4)
	2.879(4)	2.859(4)	2.701(3)	2.745(3)	2.703(3)	2.711(3)	2.713(3)	2.717(3)
	2.325(4)	2.319(4)	2.360(4)	2.362(4)	2.376(4)	2.371(4)	2.381(4)	2.378(4)
	2.890(4)	2.841(4)	2.692(4)	2.702(4)	2.683(4)	2.658(4)	2.654(4)	2.662(4)
	2.519(4)	2.537(4)	2.651(4)	2.633(4)	2.644(4)	2.657(4)	2.651(4)	2.648(4)
	2.360(4)	2.329(4)	2.332(4)	2.349(4)	2.319(4)	2.339(4)	2.322(4)	2.314(4)
	2.589(4)	2.538(4)	2.485(3)	2.471(3)	2.442(3)	2.453(3)	2.451(3)	2.446(3)
Fe_1–O × 2	2.001(2)	1.998(2)	2.003(2)	1.996(2)	1.984(2)	1.984(2)	1.982(2)	2.015(2)
(W_1–O) × 2	1.986(2)	1.997(2)	1.991(2)	1.998(2)	1.989(2)	1.985(2)	1.989(2)	1.999(2)
× 2	1.983(2)	1.959(2)	1.964(2)	1.957(2)	1.955(2)	1.956(2)	1.931(2)	1.939(2)
Average	1.990(2)	1.985(2)	1.986(2)	1.984(2)	1.976(2)	1.975(2)	1.967(2)	1.984(2)
Fe_2–O × 2	2.000(2)	2.005(2)	1.978(2)	1.987(2)	1.992(2)	1.994(2)	1.997(2)	1.975(2)
(W_2–O) × 2	1.997(2)	1.987(2)	1.981(2)	1.977(2)	1.986(2)	1.984(2)	1.976(2)	1.965(2)
× 2	2.008(2)	1.999(2)	2.006(2)	2.007(2)	2.007(2)	1.998(2)	2.028(2)	2.020(2)
Average	2.001(2)	1.997(2)	1.988(2)	1.990(2)	1.995(2)	1.989(2)	2.000(2)	1.986(2)
O_1–Fe_1–O_2	90.2(1)	91.0(1)	90.6(1)	91.9(1)	93.8(1)	93.9(1)	93.9(1)	90.5(1)
O_1–Fe_1–O_3	90.3(1)	90.3(1)	91.9(1)	90.3(1)	91.4(1)	90.9(1)	91.4(1)	90.4(1)
O_2–Fe_1–O_3	92.1(1)	91.9(1)	90.2(1)	90.8(1)	90.3(1)	90.3(1)	90.8(1)	90.5(1)
O_1–Fe_2–O_2	90.9(1)	90.2(1)	91.6(1)	90.9(1)	92.9(1)	93.0(1)	93.3(1)	90.6(1)
O_1–Fe_2–O_3	91.1(1)	91.8(1)	90.0(1)	92.1(1)	91.9(1)	91.8(1)	90.7(1)	92.3(1)
O_2–Fe_2–O_3	92.8(1)	93.3(1)	91.4(1)	92.0(1)	91.6(1)	91.3(1)	91.9(1)	91.7(1)
Fe_1–O_1–Fe_2	153.2(1)	152.4(1)	153.2(1)	152.4(1)	154.5(1)	154.6(1)	154.9(1)	150.7(1)
Fe_1–O_2–Fe_2	157.7(1)	156.2(1)	154.5(1)	153.3(1)	150.9(1)	151.0(1)	150.9(1)	153.6(1)
Fe_1–O_3–Fe_2	155.8(1)	153.7(1)	153.6(1)	153.6(1)	153.1(1)	153.6(1)	152.3(1)	152.6(1)

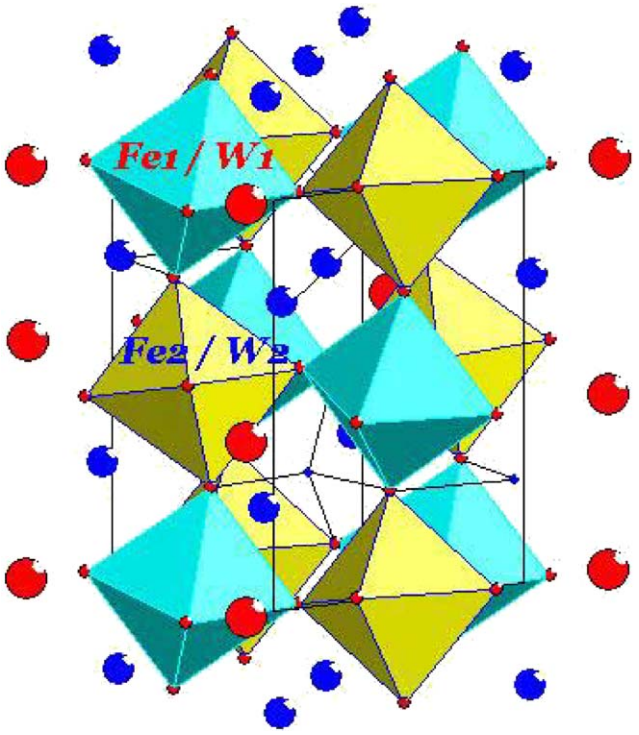

Fig. 4. The monoclinic perovskite structure of $Ca_3Fe_2WO_9$.

Table 3
Octahedral tilt angles of CFWO at different temperatures

T (K)	Fe_1/W_1		Fe_2/W_2	
	Φ	ψ	Φ	ψ
10	10.2	13.7	10.3	13.8
300	10.1	13.6	10.2	13.5
500	9.8	13.3	9.9	13.1

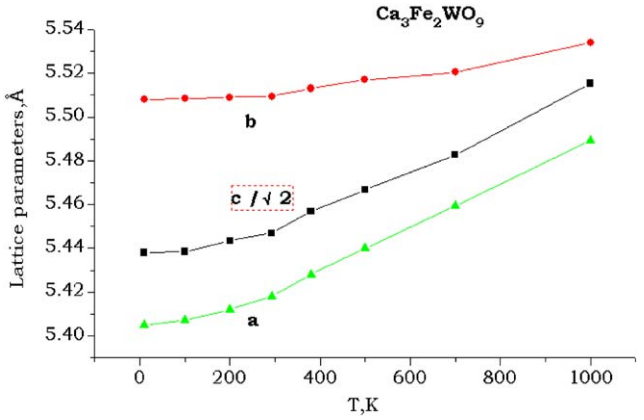

Fig. 5. Temperature dependence of lattice parameters for $Ca_3Fe_2WO_9$.

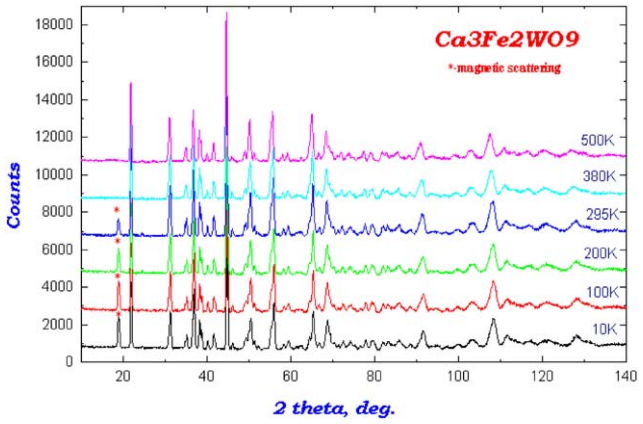

Fig. 6. Temperature evolution of NPD patterns of $Ca_3Fe_2WO_9$ (the magnetic reflections are indicated by *).

notice is that below T_{CM} there are no further changes in the NPD patterns except for a progressive increase in intensity of the magnetic reflections. This indicates that the magnetic structure remains stable across the temperature range 10–300 K. The NPD patterns of CFWO at 300, 200, 100 and 10 K were refined for two phase models, namely the nuclear phase (space group $P2_1/n$) and the magnetic phase (space group $P1$), simultaneously. The variable parameters for refinement of magnetic structure were the magnitudes and canting angles. No other structural model could be found to describe the nuclear structure, and at the same time account for the existence of two B-type sub-lattices, which is needed for the realisation of ferrimagnetic ordering. A ferrimagnetic structure was modeled with magnetic moments at the Fe positions. After Rietveld refinement, including the magnetic moment (both magnitude and orientation) a magnetic R-factor (R_{mag}) around 4% was reached. Magnetic moments were refined along each of the crystallographic axes and produced a significantly better fit to the data when refined in the c-direction. The ordered moment was constrained to lie along the c-axis, but a small component (in the frame of one standard deviation) along the a- and b-axis is also likely taking the resolution of our data into account. Values of the refined magnetic moments of the B_1- and B_2-sites are shown in Table 1. The observed moments are related to the anti-site disorder and could be evaluated for the simplest ferrimagnetic arrangements between Fe_1 and Fe_2 sub-lattices, which produce a net magnetisation, $M_s = m_{BFe1} - m_{BFe2}$ (see Fig. 7).

The magnetic structure of CFWO is consistent with the presence of a long-range cation order. The partial ordering of Fe and W into B-sites of the perovskite reduces the number of magnetic nearest-neighbour (nn) pair, whilst increasing the number of magnetic next-nearest-neighbour (nnn) pair. In our case nnn interaction probably dominates. This is spin ordering adopted by the title compound, involving a path defined by Fe–O–W–O–Fe, in which the oxygen atoms involved occupy the axial vertices of the WO_6 octahedra.

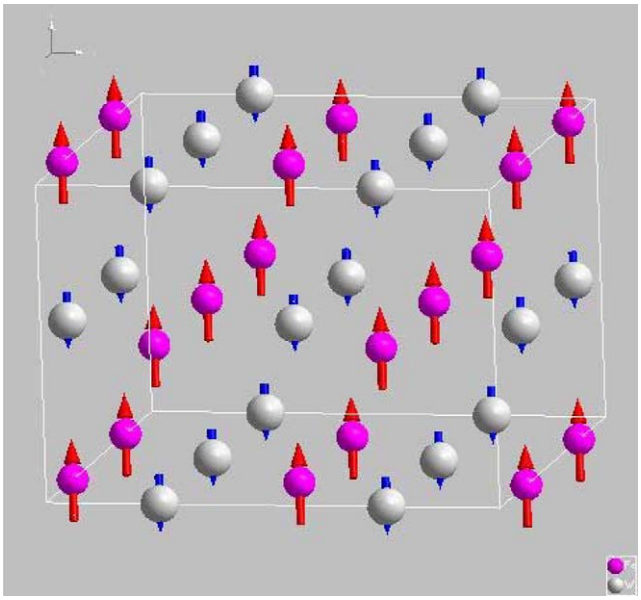

Fig. 7. A plausible model for the magnetic structure of $Ca_3Fe_2WO_9$. Diamagnetic ions are omitted.

4. Discussion

The refined atomic coordinates and bond distances for CFWO (see Tables 1 and 2) confirm the basic structural features of the proposed monoclinic perovskite structure. Fe and W were found to occupy the ($2c$) and the ($2d$) sites with different probability. The average Fe_1–O bond length is very similar to that found in other oxides with Fe^{3+} [9–13] and close to the Fe^{3+}–O length (2.045 Å) calculated from Shannon's ionic radii [25] for a high spin electron configuration in an octahedral field. The Fe–O–Fe superexchange pathways are strongly deviated from linear (the Fe–O–Fe angle is about 154°). The observed magnetic moments of Fe are smaller than what is expected for Fe^{3+} (5.9 μ_B). In order to get some insight into the cation distribution, we carried out a bond-valence calculation by means of the Brown model [26], which gives a relationship between the formal valence of a bond and the corresponding bond length. In non-distorted structures, the bond-valence sum rule states that the valence of the cation (V_i) is equal to the sum of the bond valences (v_{ij}) around this cation. The departure from this rule is a measure of the existing distortion in the bonds and indicates the presence of covalent bonding. From individual cation–anion distances the valences of the cations were calculated. The Fe_1 and Fe_2 cations exhibit valences 3.33(1) and 3.16(1) (see Table 4), slightly different from that expected in this compound, which is +3. In compensation, the valence of the W cation is somewhat lower than +6. Following the results of Mössbauer measurements we can conclude that Fe cations formally have +3 valence in both oxygen environments.

Two major factors will determine the arrangement of different cations at the B-sites in the perovskite structure.

Table 4
Distortion of polyhedra (δ) and valences ($\sum S_{ij}$) for cations in the $Ca_3Fe_2WO_9$ at the different temperatures

Cation		500 K	300 K	200 K	100 K	10 K
Ca	δ ($\times 10^{-4}$)	104.6	115.7	115.2	115.4	118.6
	$\sum S_{ij}$		2.02(1)			
Fe_1	δ ($\times 10^{-4}$)	0.67	0.57	0.45	1.72	2.81
	$\sum S_{ij}$		3.33(1)			
W_1	δ ($\times 10^{-4}$)	0.67	0.57	0.45	1.72	2.81
	$\sum S_{ij}$		5.19(1)			
Fe_2	δ ($\times 10^{-4}$)	0.39	0.18	0.083	1.13	1.49
	$\sum S_{ij}$		3.16(1)			
W_2	δ ($\times 10^{-4}$)	0.39	0.18	0.083	1.13	1.49
	$\sum S_{ij}$		4.95(1)			

Table 5
Crystallographic and magnetic properties of different $A_3Fe_2WO_9$ (A = Ba, Pb, Sr, Ca) with perovskite structure (from our data and results published in [15,16])

Cation A^{2+}	r_{ion} (Å)	Space group at 300 K	$a_p = V/z$ (Å)	T_{CM} (K)	T_{CE} (K)	Properties
Ba	1.61	$P63/mmc$	4.080	330	573	AFE–WFM (order)
Pb	1.49	$Pm3m$	3.978	340	180	FE–AFM (disorder)
Sr	1.44	$I4/m$	3.944	373	473	AFE–WFM (partial order)
Ca	1.34	$P12_1/n1$	3.859	340	—	AFE?–WFM (partial order)

Note: FE—ferroelectric; AFE—antiferroelectric; WFM—weak ferromagnetic; AFM—antiferromagnetic.

The ions can be either ordered or statistically distributed (disordered), and the controlling factors are the difference in ionic charge and in ionic size [22]. It has been shown [5,14] that the magnetic properties of complex perovskites are strongly dependent on B-site ordering. The ionic radii of Fe^{3+} and W^{6+} are similar and therefore we may say that this combination of cations in general favours a disordered arrangement.

It is interesting to note that some other oxides $A_3Fe_2WO_9$ (A = Ba, Pb, Sr, Ca) with perovskite structure also show magnetic properties [11–13] (see Table 5). It is very important to understand the possible influence of the A cations on the T_{CM} values. It is not possible to find a simple explanation for different values of T_{CM} for these perovskites based only on crystallochemical considerations using the tolerance factor t, lattice distortions, and the pseudo-cubic lattice constant a_p. Additional detailed structural investigations of complex metal oxides with different A-site cations would be necessary in order to clarify any possible correlations. Replacing Sr with Ca clearly reduces the tolerance factor and increases the octahedral tilting. Within the $A_3Fe_2WO_9$ series this process leads to a change of tilt system. It is seen that the temperature of magnetic phase transition of all the samples is nearly the same showing that the temperature of magnetic ordering is insensitive to the change of A-site composition. This is in good agreement with band structure calculations on double perovskites that contain B'' cations such as W^{6+}. The substitution at the A-site does not change the band gap significantly [28].

But by analogy with $LnFeO_3$ compounds [27] we may assume that T_{CM} is strongly related with the value of the Fe–O–Fe angle and with lattice distortions. At the same time, it is clear now that the lattice distortions and the degree of crystallographic order/disorder at the Fe-sites and/or the oxygen deficiency should be varied properly with the type of A-cations.

It is also well known that the differences in the valence and size between the B' and B'' cations in double perovskite-type compounds are crucial in controlling the physical properties. The actual degree of Fe/W order depends on the synthesis conditions and as a rule an increased order may be obtained with increased synthesis temperature or treatment time [29,30].

5. Concluding remarks

We have revised some experiments that may provide the key ingredients for a clear understanding of the magneto-electric properties of CFWO.

The monoclinic perovskite CFWO was synthesised and structurally characterised using the Rietveld analysis of NPD data at different temperatures. The partial ordering of Fe and W cations into two different B-sites (2c) and (2d) was determined. The precise metal–oxygen distances, derived from NPD data, allowed us to calculate the cation valences and their distortion polyhedra. The monoclinic superstructure of CFWO arises from the combination of partial cation ordering and from a tilt of the BO_6 octahedra. Below T_{CM}, the magnetic structure, charac-

terised by a propagation vector $k = (1/2, 1/2, 0)$, develops and accounts for some additional reflections of magnetic origin. According to the proposed model for the magnetic structure it can be described as an array of (20−1) layers showing ferromagnetic order. The layers couple antiferromagnetically to each other and the Fe moments are aligned along the *c*-axis.

Structural and magnetic features of CFWO are considered and compared with those of some other quaternary complex oxides with perovskite-related structure. It must be admitted that the question of possible ferro- or antiferroelectric state in CFWO is still an open question and the dielectric properties need further consideration.

Acknowledgments

The present work has been supported by the Royal Swedish Academy of Sciences, which is gratefully acknowledged. We thank Prof. P. Svendlindh and Dr. V. Stanciu from the University of Uppsala for help with the magnetic measurements and Dr. V. Shagdarov from Moscow State University for his help with the Mössbauer experiment.

References

[1] N.A. Hill, A. Filippetti, J. Magn. Magn. Mater. 242 (2002) 976.
[2] A. Filippetti, N.A. Hill, Phys. Rev. B 65 (2002) 195120.
[3] H. Schmid, Ferroelectrics 162 (1994) 317.
[4] E.V. Wood, A.E. Austin, Int. J. Magn. 5 (1974) 303.
[5] A.J. Freeman, H. Schmid (Eds.), Magnetoelectric Interaction Phenomema in Crystals, Gordon and Breach, New York, 1975, p. 228.
[6] Yu.N. Venevtsev, V.V. Gagulin, Ferroelectrics 162 (1994) 23.
[7] G.A. Smolensky, I.E. Chupis, Sov. Phys. -Uspekhi 25 (1982) 475.
[8] G. Blasse, J. Inorg. Nucl. Chem. 27 (1995) 993.
[9] Yu.N. Venevtsev, E.D. Politova, S.A. Ivanov, Ferro- and Antiferroelectrics of Barium Titanate Family, Chemistry, Moscow, 1985, p. 256 (in Russian).
[10] S.A. Ivanov, S.G. Eriksson, N.W. Thomas, R. Tellgren, H. Rundlof, J. Phys.: Condens. Matter 13 (2001) 25.
[11] S.A. Ivanov, S.G. Eriksson, R. Tellgren, H. Rundlof, Mater. Res. Bull. 36 (2001) 2585.
[12] S.A. Ivanov, S.G. Eriksson, R. Tellgren, H. Rundlof, Mater. Res. Bull. 39 (2004) 615.
[13] S.A. Ivanov, S.G. Eriksson, R. Tellgren, H. Rundlof, Mater. Res. Bull. 39 (2004) 2317.
[14] V.V. Ivanova, A.G. Kapyshev, Yu.N. Venevtsev, Inorg. Mater. 6 (1970) 168.
[15] E.G. Fesenko, V.S. Filipiev, M.F. Kupriyanov, Inorg. Mater. 6 (1970) 179.
[16] J. Rodriguez-Carvajal, Physica B 192 (1993) 55.
[17] G. Long (Ed.), Mössbauer Spectroscopy Applied to Magnetism and Materials Science, Plenum Press, New York, 1993, p. 161.
[18] G. Long (Ed.), Mössbauer Spectroscopy Applied to Inorganic Chemistry, Plenum Press, New York, 1987, p. 507.
[19] A. Altomare, C. Giacovazzo, A. Guagliardi, G.G. Moliterni, R. Rizzi, P.E. Werner, J. Appl. Crystallogr. 33 (2000) 1180.
[20] R. Mitchell, Perovskites: Modern and Ancient, Almaz Press, Canada, 2003.
[21] P.M. Woodward, Acta Crystallogr. B 53 (1997) 32.
[22] W.A. Groen, F.P.F. van Berkel, D.J.W. Ijdo, Acta Crystallogr. C 42 (1986) 1472.
[23] K. Uchino, S. Nomura, Ferroelectrics 17 (1978) 505.
[24] M.A. Gileo, J. Phys. Chem. Solids 13 (1960) 33.
[25] R.D. Shannon, Acta Crystallogr. A 32 (1976) 751.
[26] I.D. Brown, in: M.O. Keefe, A. Navrotsky, (Eds.), Structure and Bonding in Crystals, vol. 2, Academic, New York, p. 1.
[27] D. Trevez, M. Fibchutz, P. Coopens, Phys. Lett. 18 (1965) 126.
[28] H.W. Eng, P.W. Barnes, B.M. Auer, P.M. Woodward, J. Solid State Chem. 175 (2003) 94.
[29] P.M. Woodward, R.D. Hoffman, A.W. Sleight, J. Mater. Res. 9 (1994) 2118.
[30] D. Sanchez, J.A. Alonso, M. Garcia-Hernandez, M.J. Martinez-Lope, J.L. Martinez, Phys. Rev. B 65 (2002) 104426.